Sequential, X-ray-induced Single-crystal-to-single-crystal Transformation followed by Topotactic Reduction in a Potassium Crown Ether Complex of Tetrachloroaurate(III)

Navpreet K. Sethi, Adrian C. Whitwood and Duncan W. Bruce*

Department of Chemistry
University of York
Heslington
YORK YO10 5DD (UK)
Tel: (+44) 1904 324085
E-mail: duncan.bruce@york.ac.uk

Introduction

Single crystal X-ray crystallography is a well-established technique that has long been used to determine crystal and molecular structures of compounds that are often products of reactions. Powerful though this is, it has for the most part been a 'static' tool inasmuch as the compounds of interest are stable materials whose transformation is complete at the time that the structure is solved.

More recently, however, reports have appeared of solid-state reactions, studied by X-ray crystallography, where it has been possible to observe the reactants and then the products, the latter formed through the intervention of some external stimulus. Thus, in an excellent review of the field in 2014, Hatcher and Raithby[1] detailed a series of transformations initiated in single crystals and followed by high-speed crystallography at synchrotron sources. Interesting examples include single-crystal-to-single-crystal (SCSC) transformations consequent on dehydration where there is a dramatic effect on magnetic properties,[2] SCSC transition that modify the emissive properties of 2,4-trifluoromethylquinolines[3] and SCSC transitions to create porous polymers by photopolymerization of anthracene units attached to a triptycene scaffold and taking advantage of the pre-organization afforded by the single-crystal form.[4] In addition, there are the reports of solid-state SCSC reactivity from Weller and co-workers[5] relating to the formation of σ-alkane complexes of rhodium(I) obtained by treating single crystals of the $[Rh(d^{i}bpe)(nbd)]^{+}$ cation ($dpp^{i}b$ is 1,2-bis(di-*iso*-butylphosphino)ethane and nbd is norbornadiene) with gaseous hydrogen, which they developed with the solid-state organometallic chemistry of with related systems.[6]

Reports of SCSC transitions initiated by X-rays are rare, for example, the transformation of a *syn*-tricyclo[4.2.0.$0^{2,5}$]octane to a (*Z, Z*)-cycloocta-1,5-diene derivative[7] and also related substrates,[8] as well as of an X-ray-induced electron-transfer-coupled spin transition in a cyanide-bridged Fe–Co molecular square.[9]

However, to the best of our knowledge and excluding transformations that involve a change in electronic structure (*e.g.* spin crossover, valence tautomerism), X-rays have not previously been as sole stimulus responsible for a single-crystal-to-single-crystal transformation in a discrete coordination complex at a constant cryogenic temperature.

As part of a wider study aimed at the preparation of well-defined, heterobimetallic coordination complexes,[10] we reported the single crystal structure of the [K(18-crown-6)]$^+$ salt of a material containing, in different proportions, the anions $[Cl_3Pd(\mu\text{-}Cl)_2PdCl_3]^{2-}$, $[Cl_3Pt(\mu\text{-}Cl)_2PtCl_3]^{2-}$ and $[Cl_3Pd(\mu\text{-}Cl)_2PtCl_3]^{2-}$.[11] As an extension of these studies, we prepared the new complex [K(18-crown-6)][$AuCl_4$] and found that it could be crystallized as two different polymorphs (*P*–1 or *C*2/*c*) depending on the conditions used. If the crystallization was not carried out under controlled conditions as described below, then [K(18-crown-6)][$AuCl_2$][12] was recovered instead in the $P2_1/n$ space group. During the study of these complexes by X-ray single crystal diffraction, it became apparent that the X-rays induced structural and chemical changes, the results of which are now described.

Results and Discussion

[K(18-crown-6)][$AuCl_4$] was isolated from the room-temperature reaction of K[$AuCl_4$] with [18-crown-6] in either water or aqueous acetic acid and the precipitate obtained was crystallized from CH_2Cl_2 (under N_2, 5 °C, dark) giving the complex as crystals in the *C*2/*c* space group (**1**). However, single crystals in the *P*–1 space group (**2**) could be obtained directly from reactions carried out in aqueous acetic acid as well by recrystallisation from CH_2Cl_2. While both polymorphs could be obtained from CH_2Cl_2, it was not possible to determine a protocol to favor one over the other and the *P*–1 polymorph was obtained on most occasions. Furthermore, in obtaining the *P*–1 polymorph, it was observed that if the crystallization is not carried out at sub-ambient temperature and under an inert atmosphere, then a mixture of [K(18-crown-6)][$AuCl_2$] (minor product) and [K(18-crown-6)][$AuCl_4$] (major product) is obtained. On the other hand, if the crystallization is carried out at room temperature, in air and in the presence of light, [K(18-crown-

6)][$AuCl_2$] is observed exclusively (**3**). Interestingly, the crystal structure of [K(18-crown-6)][$AuCl_4$] has not been reported before, but previous attempts to isolate it from a mixture of K[$AuCl_4$] and [18-crown-6] in MeOH followed by crystallization from a MeOH/Et_2O mixture, led to colorless crystals of [K(18-crown-6)][$AuCl_2$].[12] These observations suggest *in situ* photoreduction of gold(III) to gold(I) that is promoted thermally.

It was then observed that while collecting data for the *P*–1 polymorph (note that all data collections reported in the paper were at 110 K), the data quality declined significantly with time both in terms of r_{int} and the fit of reflections to predicted positions. Therefore, a rapid data collection was undertaken (with Mo radiation) for the *P*–1 polymorph. Then, in a subsequent data collection again with Mo radiation, a crystal of the *P*–1 polymorph was held in the X-ray beam and data collected over an extended period. Analysis of the first 92 frames of the extended data collection (6798 reflections, 1 hour 25 minutes exposure to the X-ray beam) corresponded to the expected *P*–1 structure whilst analysis of the last 100 frames (2424 reflections, 15 hours 5 mins exposure at the start of these frames) gave the structure of the *C*2/*c* polymorph. Furthermore, in analyzing the data obtained after the 15-hour exposure, it became apparent that they could not be modelled satisfactorily with only tetrachloroaurate(III) and that residual electron density suggested the presence of $[AuCl_2]^-$ anions. The structures obtained from these data collections are now described.

Crystal and Molecular Structure of [K(18-crown-6)][$AuCl_4$] in P*–1*

In order to describe the observed changes, the structure of the *P*–1 polymorph is first described. As noted above, two data sets were recorded. In the first determination (**2a**), 17338 reflections were collected with 15 s frames, allowing complete data collection in 69 min, while data for the second (**2b**) where the first 6798 reflections (collected in 85 min) of a longer data collection in which the *P*–1 to *C*2/*c* transformation was studied. The complex possesses an ordered structure with a large asymmetric unit (Fig. 1 – all representations from the **2b** data set) and unit cell

Table 1 Crystal data for [K(18-crown-6][$AuCl_4$] and [K(18-crown-6][$AuCl_2$]

	1a	**1b**	**1c**	**2a**	**2b**	**3**
CCDC Ref. No.	1823620	§	1823619	1823621	§	1823622
Molecular Formula	(K[18-crown-6]) [$AuCl_4$]	(K[18-crown-6]) 0.63[$AuCl_4$] 0.37[$AuCl_2$]	(K[18-crown-6]) 0.86[$AuCl_4$] 0.14[$AuCl_2$]	(K[18-crown-6]) [$AuCl_4$]	(K[18-crown-6]) [$AuCl_4$]	(K[18-crown-6]) [$AuCl_2$]
Empirical formula	$C_{12}H_{24}AuCl_4KO_6$	$C_{12}H_{24}Au0.97Cl_{3.14}KO_6$	$C_{12}H_{24}AuCl_{3.7}KO_6$	$C_{12}H_{24}AuCl_4KO_6$	$C_{12}H_{24}AuCl_4KO_6$	$C_{12}H_{24}AuCl_2KO_6$
Formula weight / g mol^{-1}	642.18	605.69	631.67	642.18	642.18	571.21
T / K	110	110	110	110	110	110
Length of data collection/min	14	85	68	28	905	120
Wavelength (Å)	0.7107 (MoK_α)	0.7107(MoK_α)	(1.54184) (CuK_α)	0.7107(MoK_α)	0.7107(MoK_α)	0.7107(MoK_α)
Crystal system	monoclinic	monoclinic	monoclinic	triclinic	triclinic	monoclinic
Space group	*C*2/c	*C*2/*c*	*C*2/*c*	*P*–1	*P*–1	$P2_1/n$
Colour	yellow	yellow	yellow	yellow	yellow	colourless
Shape	irregular	irregular	irregular	irregular	irregular	plate
Unit cell dimensions /Å	*a* = 13.9553(10) *b* = 11.3990(5) *c* = 14.2151(9)	*a* = 13.8702(18) *b* = 11.5709(12) *c* = 14.427(2)	*a* = 13.8995(7) *b* = 11.4692(5) *c* = 14.3259(7)	*a* = 9.0720(14) *b* = 14.7628(14) *c* = 24.597(4)	*a* = 9.0592(5) *b* = 14.7606(8) *c* = 24.6225(15)	*a* = 8.7731(12) *b* = 7.9309(11) *c* = 13.8621(19)
α / °	90	90	90	98.807(12)	98.815(5)	90
β / °	108.659(7)	109.396(18)	109.088(5)	94.557(14)	94.425(5)	103.837
γ / °	90	90	90	96.294(11)	96.293(5)	90
Volume / $Å^3$	2142.4(2)	2184.1(5)	2158.21(19)	3220.2(8)	3219.2(3)	936.5(2)
Z	4	4	4	6	6	2
ρ_{calc} / Mg m^{-3}	1.991	1.842	1.944	1.987	1.988	2.026
Absorption coefficient/mm^{-1}	7.582	7.130	18.951	7.567	7.569	8.3838
F(000)	1240.0	1172.0	1220.0	1860.0	1860.0	552.0
Crystal size / mm^3	0.3499 × 0.2175 × 0.0974	0.1682 × 0.1157 × 0.0525	0.212 × 0.158 × 0.084	0.1354 × 0.0828 × 0.059	0.1682 × 0.1157 × 0.0525	0.20 × 0.14 × 0.05
2θ range for data collection	6.86 to 64.24°	6.23 to 60.76°	10.24 to 134.148°	6.06 to 55.7°	6.06 to 61.2°	5.02 to 56.68°
Index ranges	-20 ≤ h ≤ 10, -16 ≤ k ≤ 15, -16 ≤ l ≤ 20	-18 ≤ *h* ≤ 4, -14 ≤ *k* ≤ 8, -17 ≤ *l* ≤ 14	-16 ≤ *h* ≤ 16, -13 ≤ *k* ≤ 10, -14 ≤ *l* ≤ 17	-11 ≤ h ≤ 10, -15 ≤ k ≤ 19, -24 ≤ l ≤ 29	–5 ≤ *h* ≤ 12, –9 ≤ *k* ≤ 19, –32 ≤ *l* ≤ 10	–11 ≤ *h* ≤ 11, –10 ≤ *k* ≤ 10, –18 ≤ *l* ≤ 18
Reflections collected	5504	2424	5747	17338	6798	9414
Independent reflections	3328 [$R_{(int)}$ = 0.0382]	1821 [$R_{(int)}$ = 0.0266]	1930 [$R_{(int)}$ = 0.0381]	12417 [$R_{(int)}$ = 0.0464]	6628 [$R_{(int)}$ = 0.0101]	2334 [$R_{(int)}$ = 0.0537]
Completeness to θ = 28.30°	98.85	62.51	99.9 (to θ = 67.07°)	98.65	39.44	99.7
Max. and min. transmission	0.546 & 0.203	0.711 & 0.523	0.306 & 0.065	0.688 & 0.541	0.591 & 0.429	0.658 & 0.368
Data / restraints / parameters	3328/0/154	1821/64/150	1930/13/174	12417/108/652	6628/84/652	2334/0/104
Goodness-of-fit on F^2	0.996	1.099	1.073	1.072	1.215	0.988
Final *R* indices [$I > 2\sigma(I)$]	R_1 = 0.0398, wR_2 = 0.0654	R_1 = 0.0875, wR_2 = 0.2228	R_1 = 0.0326, wR_2 = 0.0863	R_1 = 0.0671, wR_2 = 0.1291	R_1 = 0.0598, wR_2 = 0.1291	R_1 = 0.0258, wR_2 = 0.0504
R indices (all data)	R_1 = 0.0583, wR_2 = 0.0752	R_1 = 0.1097, wR_2 = 0.2411	R_1 = 0.0339, wR_2 = 0.0879	R_1 = 0.0951, wR_2 = 0.1527	R_1 = 0.0679, wR_2 = 0.1345	R_1 = 0.0438, wR_2 = 0.0561
Largest diff. peak and hole/e $Å^{-3}$	0.83 & –1.19	2.08 & –0.57	1.43 & -0.79	4.02 & –2.46	1.91 & –1.28	1.235 & -0.744

§ In each case, the parameters come from a partial data set extracted from the long data collection (see text).

parameters for the two collections agree to better than 1%, with the latter furnishing a slight better value for R_1 (6.71% *vs* 5.98%). It is interesting that the largest thermal ellipsoids from the latter data set are found on the chloride ligands, in particular those in the notionally *trans*-bridging positions.

The structure shows square-planar tetrachloroaurate(III) ions bridging potassium crown ether units to give a polymeric structure (Fig. 1); the bridges take two forms. The first, which occurs with twice the frequency of the other, has two *cis*-chloro ligands (Cl9 and Cl10) binding to potassium ions held in adjacent crown ethers (Fig. 2a). Here, all of the interionic distances (Table S1) are less than the sum of the van der Waals radii for K^+ (1.65 Å) and Cl^- (1.67 Å). The second bridging motif is altogether quite different (Fig. 2b), being much more unsymmetric and with none of the interionic distances shorter than the sum of the van der Waals radii (Table S2).

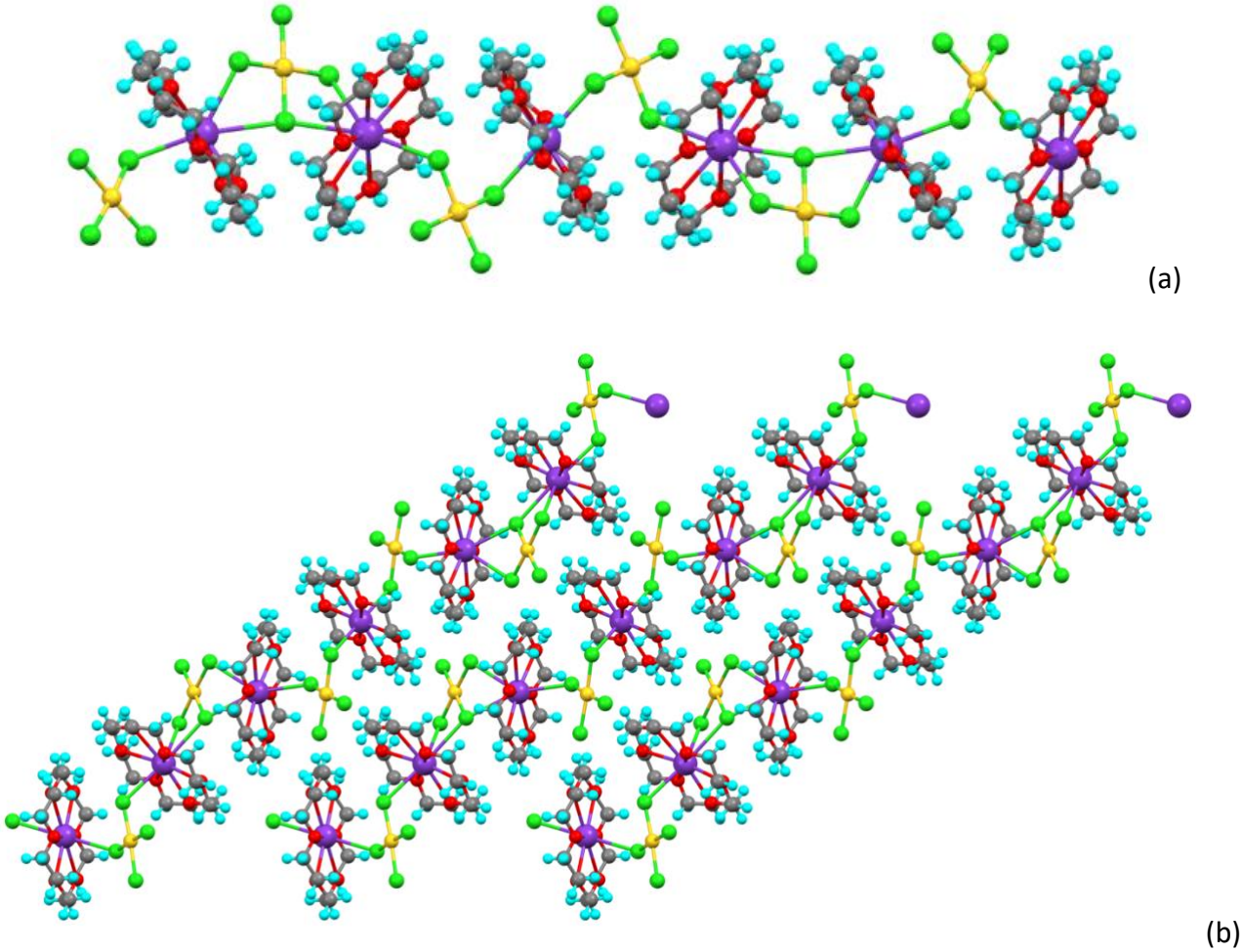

Figure 1. The *P*–1 polymorph of [K(18-crown-6)][$AuCl_4$] (**2b**): (a) asymmetric unit; (b) view down the *a*-axis showing the arrangement of adjacent polymer chains.

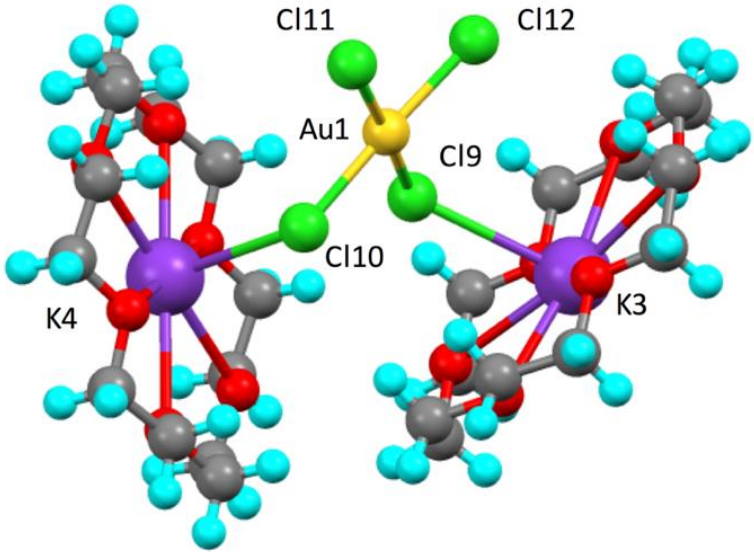

(a)

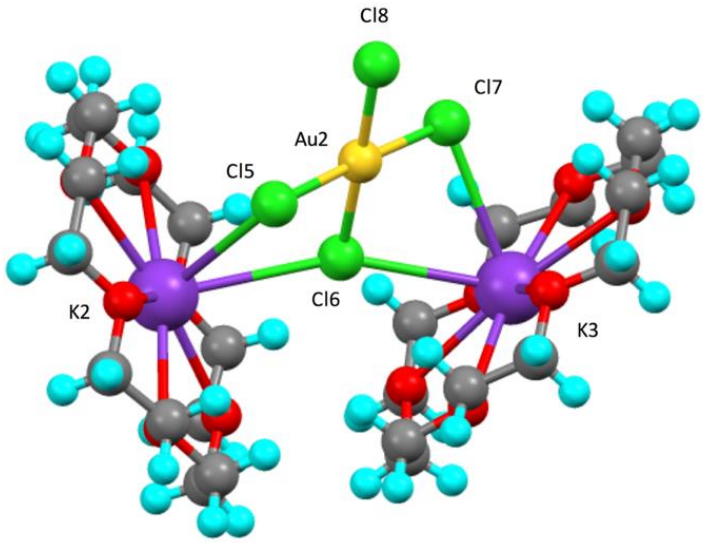

(b)

Figure 2. Part of the asymmetric unit of the *P*–1 polymorph (**2**) showing (a) the simple, prevalent *cis*-chloro bridge between two $[K(18\text{-crown-6})]^+$ cations and (b) the more complicated and less common *trans*-chloro bridge. Atom labels are consistent with the cif file.

Crystal and Molecular Structure of [K(18-crown-6)][AuCl$_4$] in C2/c

This time, three data sets were studied. The first (**1a**) arose from a crystal obtained from dichloromethane where 5504 reflections were collected, whereas the second (**1b**) was based on data collected after 15 hours of irradiation of the *P*–1 polymorph in the X-ray beam and was from the same data collection as that of **2b**. In this case, there are differences in the unit cell

parameters as well as in the final values for R_1 (3.98% *vs* 8.75%, respectively). In a third experiment, the crystal with the *P*–1 space group was first irradiated for 2.5 hours using more intense copper radiation leading to conversion to the C2/c polymorph prior to collection of a full dataset. The dataset showed the presence of both the tetrachloroaurate(III) (86%) and dichloroaurate(I) anions (14%) (**1c**) with R_1 = 3.26% (*vide infra*). Discussion of the structure of the *C*2/*c* polymorph uses data from **1a** which does not contain any discernible amount of the Au(I) complex.

The major difference between the *C*2/*c* and *P*–1 polymorphs is the orientation of the $[AuCl_4]^-$ anions. Thus, in the *C*2/*c* structure the anion has, in effect, become disordered rotationally about an axis perpendicular to the plane containing the gold and the chloride ions (ignoring a small change in position of the gold centers of 0.43(1) Å), so that the bridges are both *cis* and *trans* between each pair of $[K(18\text{-crown-6})]^+$ cations with additional close contact to a third chloride in the *trans* case (Fig. 3). Thus, as shown in Fig. 3, the bridging pathways (Cl–Au–Cl) between the two potassium ions are *via* pairs of symmetry-equivalent chloride ligands.

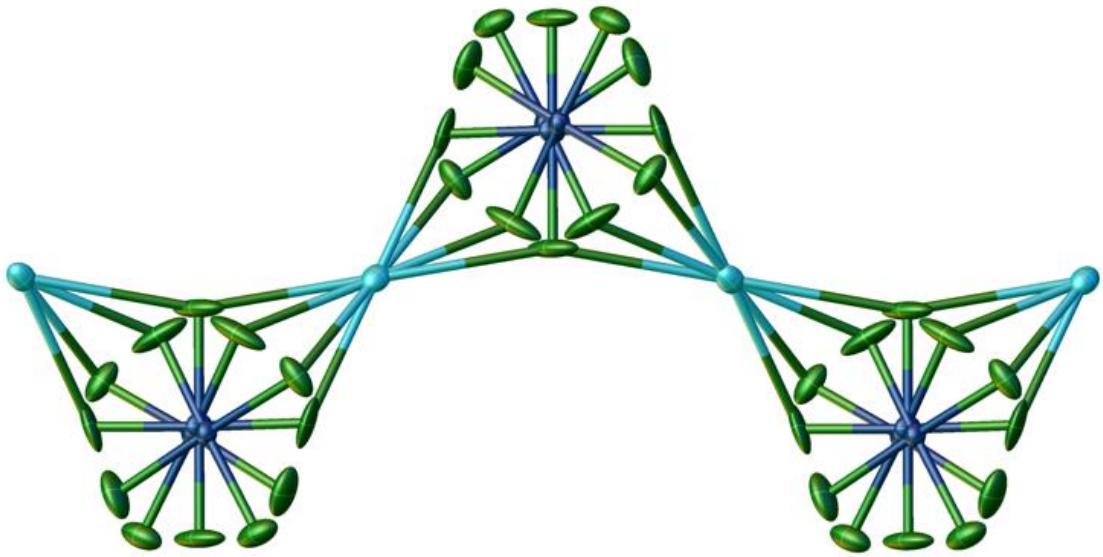

Figure 3 Representation of the disordered $[AuCl_4]^-$ bridging anion of **1** showing the *trans* and two possible *cis* bridging modes through symmetry-equivalent pairs of chloride ligands (atoms from the crown ethers are removed for clarity); distances are found in Table S2.

It is then possible to overlay the two polymorphs by fixing on the positions of potassium ions. Fig. 4a reveals fairly good overlap both of the crown ethers and of the gold in the anions confirming that the major distortions during the transition are of the orientation of the tetrachloroaurate(III) anion. That said, there are some small movements, which lead to changes in the packing of the polymer chains as shown in Figure 4(b) and (c). This is seen by viewing the structure along the axis of the polymer chain, where a hexagonal-like arrangement is seen. In the *C*2/*c* polymorph (Fig. 4c), the apparent hexagon is slightly distorted so that of the angles subtended at potassium in the pseudo-hexagonal plane, two are 98.468(5)° and four are 130.766(3)°, with $K^+\cdots K^+$ distances of 8.6334(4), and 11.3990(5) Å. In the *P*–1 polymorph (Fig. 4b) however, the outer hexagon is totally unsymmetric with internal angles of 130.814(10), 98.242(14), 130.934(11), 131.781(10), 98.586(14) and 129.633(10)° and intercolumnar distances of *ca* 8.8 Å and 11.4 Å.

Interestingly, there is a report by Caleja *et al.*[13] in which the preparation and X-ray single crystal structure of $[(H_3O)(18\text{-crown-6})][AuCl_4]$ are reported. The authors report that the salt can be crystallized as two different polymorphs – *Pbam* when obtained from aqua regia and *P*2/*m* from diluted aqua regia – and that the former polymorph is highly crystalline (*e.g.* final R_1 = 2.2%) whereas the latter is rather disordered (final R_1 = 8.71%). Indeed, they were unable to refine the *P*2/*m* polymorph to a chemically sensible model. Note that they do not describe a transformation between the two. They did, however, note that the *c* lattice parameter of the ordered polymorph (12.0284(5) Å) was very similar to the *b* lattice parameter of the disordered polymorph (12.0398(7) Å). Curiously, while in completely different space groups, the *c* lattice parameter of the *C*2/*c* polymorph (**1c**) of $[K(18\text{-crown-6})][AuCl_4]$ (14.3259(7) Å) is very similar to the *b* lattice parameter of the *P*–1 polymorph. While different salts and pairs of space groups, it is nonetheless interesting and to note some similarities in properties between these two related systems.

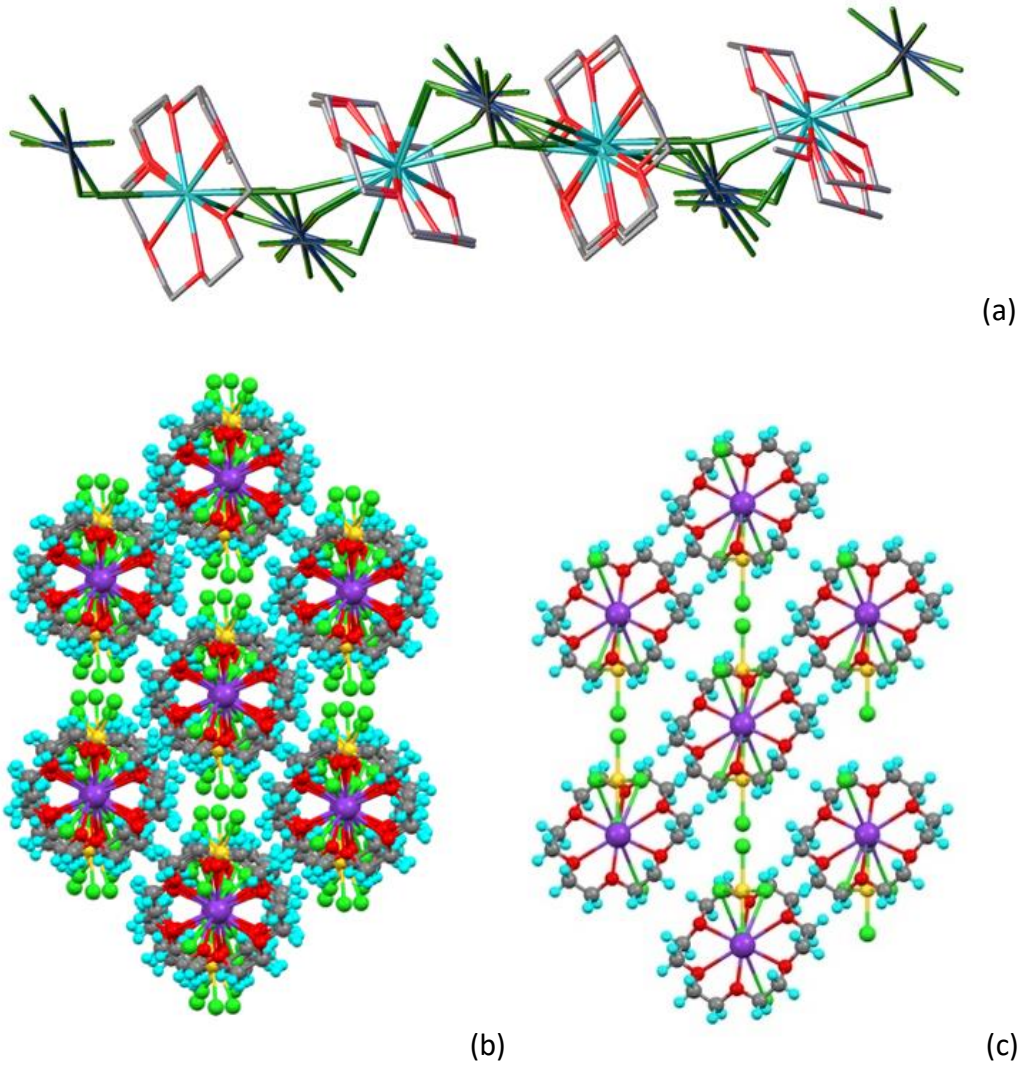

Figure 4 (a) Overlaid structures of the two polymorphs; (b) view perpendicular to the polymer chain in the *P*–1 polymorph (**2**); (c) view down the *c*-axis in the *C*2/*c* polymorph (**1** – from a modified cif file removing disorder and prepared for illustrative purposes).

Single-crystal-to-single-crystal transformation and X-ray-induced reduction

In the X-ray beam, the transformation from the *P*–1 to the *C*2/*c* polymorph was very rapid, being effectively complete within 2.5 hours. For this reason and as described above, it was not possible to collect an entire dataset for either polymorph *during* the transition. Remarkably, at the end of the experiment, the crystal was recovered apparently unchanged with no signs of damage or rupture and, furthermore, the crystal-crystal transformation was repeated several times in the X-ray beam (with a new sample on each occasion) giving the same results each time, demonstrating reproducibility. Note that the lack of disorder in the *P*–1 polymorph leads to the rather low

symmetry (different gold bridging units), whereas the disorder in the *C*2/*c* polymorph allows the symmetry to increase.

One other point of note is that there is no apparent epitaxial relationship that relates to the change from the *P*–1 to the *C*2/*c* polymorph. Superficially the data could be seen to suggest such a relationship between the *b*-axis of the *P*–1 polymorph and the *c*-axis of the *C*2/*c* polymorph, but examination of the structure shows this not to be the case.

However, in then considering both the data set collected at the end of the extended irradiation at the wavelength of MoKα (**1b**) and that for **1c** (obtained following irradiation at the wavelength of CuKα at greater intensity), it was clear that there was significant additional electron density corresponding to gold and chlorine that was not accommodated in modelling using only [K(18-crown-6)][$AuCl_4$]. Thus, modelling **1b** with only gold(III) gave R_1 = 10.54%, while for **1c** with only gold(III) R_1 = 13.17%. However, if $[AuCl_2]^-$ is included on the gold sites in **1b** at an occupancy of ≈37% then R_1 drops to 8.75%. Similarly, for **1c**, inclusion of gold(I) at an occupancy of 14% reduces R_1 to 3.26%.

Thus, it seems that following the single-crystal-to-single-crystal transformation from *P*–1 to *C*2/*c*, there is a photoreduction of the gold(III) to give [K(18-crown-6)][$AuCl_2$] with the same *C*2/*c* space group. Indeed, the transformation can be seen visibly as the single crystal retains its original yellow color (Au^{III}) at the center while being surrounded by colorless Au^{I} (Fig. 4). Since the data sets consist of a series of runs at fixed ϕ and κ but varying ω, it is possible roughly to follow the transformation by extracting reflection data from each run independently and simply varying the proportion of Au(I) and Au(III) complexes to optimize the model. This allowed an evaluation of the rate of change (Fig. 5) which is found to approximately monotonic up to *ca* 50% gold(I), by which time the crystal has degraded to the extent that the diffraction resolution has dropped from <0.71 Å to *ca* 1.1 Å. It then proved possible to extract the parameters for the Au(I) complex alone into a cif file and it is therefore instructive to compare the structures of the new (*C*2/*c*) and known (*P*2_1/*n*)[12] polymorphs.

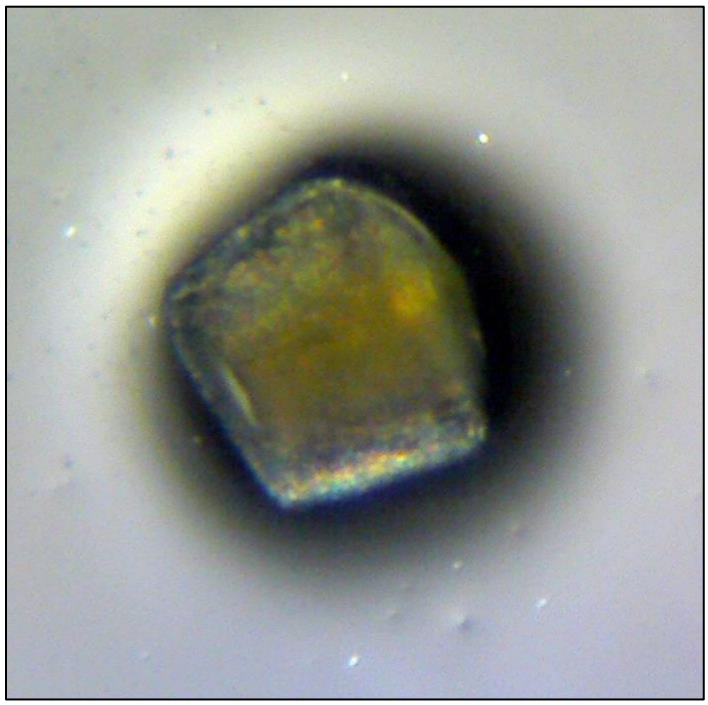

Figure 4 A single crystal of [K(18-crown-6)][$AuCl_4$] after data collection showing yellow Au^{III} surrounded by colorless Au^{I}.

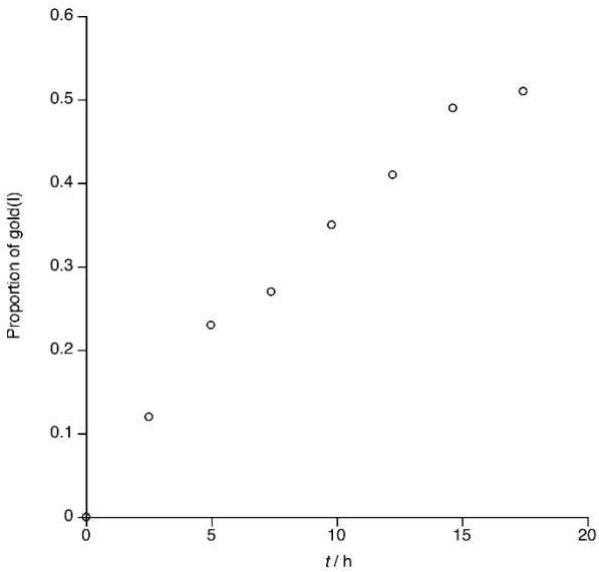

Figure 5 Plot of the evolution of gold(I) as a function of time on X-irradiation (λ = 0.7107 Å – MoKα) of a single crystal of the *P*–1 polymorph of [K(18-crown-6)][$AuCl_4$]. Note that conversion from *P*–1 to *C*2/*c* is effectively complete by the time the first data point is collected.

Crystal and Molecular Structure of the two polymorphs of [K(18-crown-6)][$AuCl_2$]

The structure of the $P2_1/n$ polymorph is described here in more detail than published originally[12] to facilitate comparison. Thus, zig-zag chains of repeating Cl–Au–Cl···K units are found with K^+ complexed by the 18-crown-6 with all chloride ligands and gold centers contained within the same plane within each chain (Fig. 6a). The Cl–Au bond lengths at 2.2637(11) Å are unremarkable, while the K^+···Cl distance, at 3.2340(12) is at the limit of the sum of the van der Waals' radii for K^+ and Cl^- and is therefore considered to be electrostatic in nature (Fig. 6b). Interestingly, we note that the X-ray single crystal structures of the copper(I)[14] and silver(I) congeners have been determined and are isostructural and isomorphous.

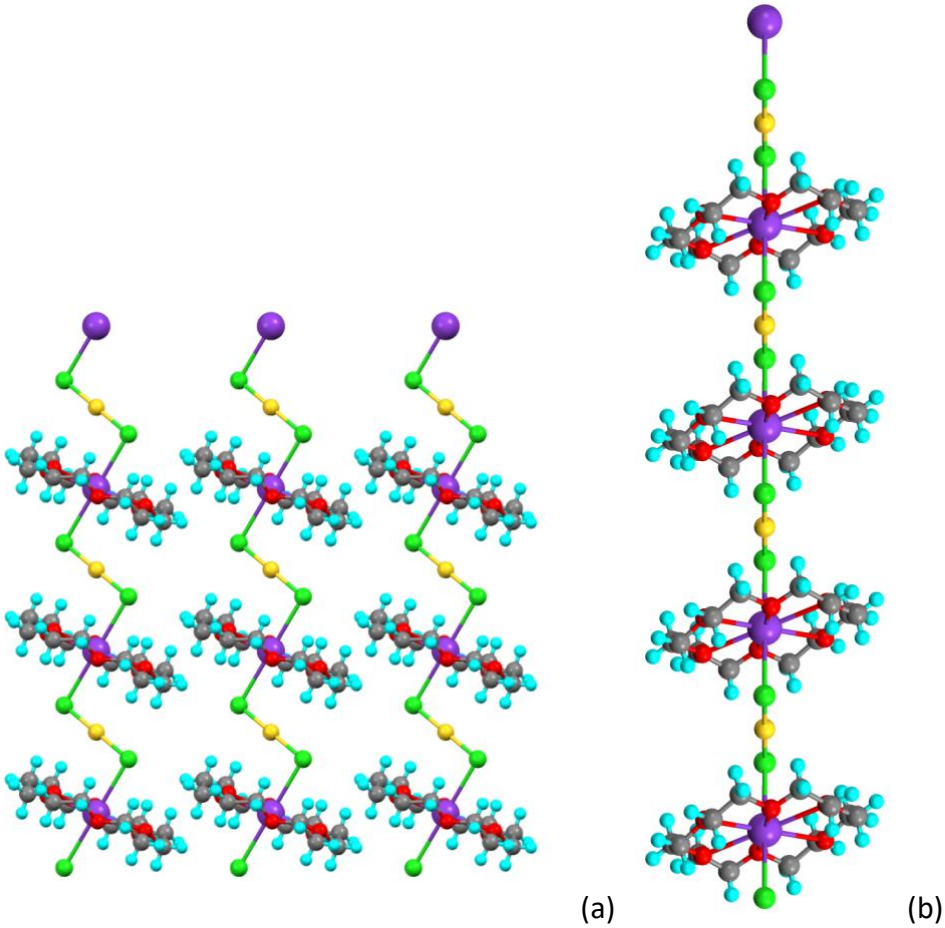

Figure 6 View of [K(18-crown-6)][$AuCl_2$]: (a) down the *c*-axis and (b) just offset from *a*-axis and showing the co-planarity of the heavy atoms ($P2_1/n$ polymorph)

Now considering the *C*2/*c* polymorph obtained by irradiation of [K(18-crown-6)][$AuCl_4$] in the same space group, the crown ether rings retain the alternating arrangement characteristic of both gold(III) polymorphs, which would be expected given the relationships through solid-state interconversion (Fig. 7). This contrasts with the co-parallel organization in $P2_1/n$ polymorph.

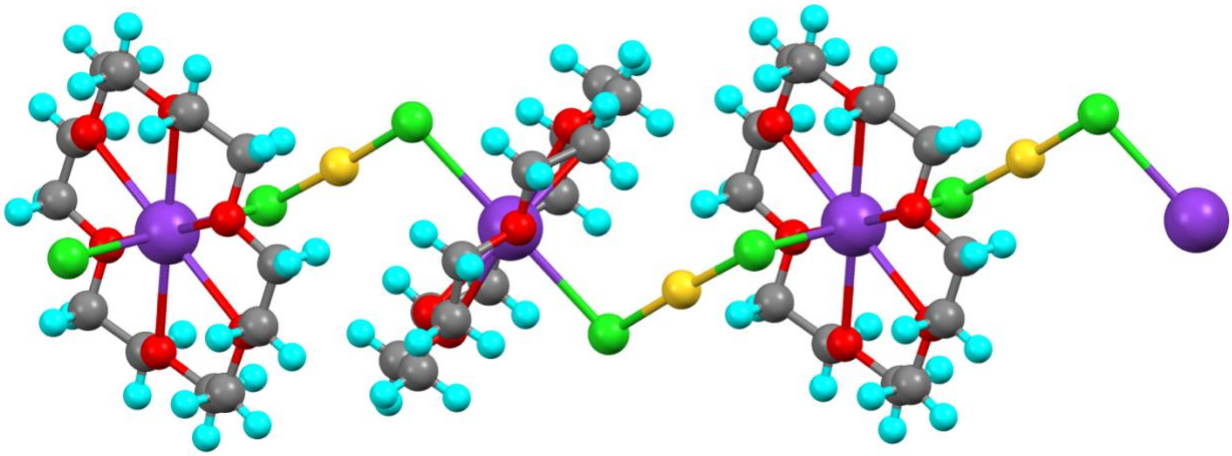

Figure 7 Structure of [K(18-crown-6)][$AuCl_2$] (**3**) in the *C*2/*c* polymorph.

Furthermore, whereas in the $P2_1/n$ polymorph all of the Cl and Au centers were found in the same plane, this is not the case in *C*2/*c* polymorph where the two linear $AuCl_2$ units either side of each potassium are all coplanar, but there is a rotation of 65.15° taking the next $AuCl_2$ unit in a different direction ($d_{Au–Cl}$ = 2.258() Å). The subsequent rotation then comes back the other way to generate a linear chain of potassium ions. The differences in the arrangement of the heavy atoms is shown also in Figure 8.

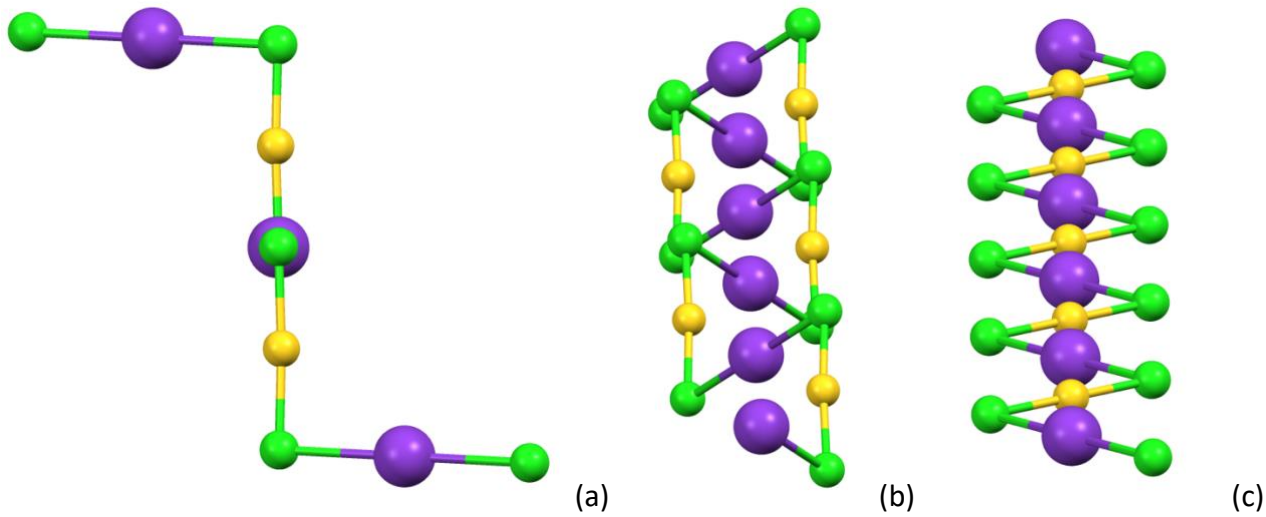

Figure 8 View of: (a) the Cl–Au–Cl···K^+ 'spine' in the *C*2/*c* polymorph of **3** looking directly along an axis containing the linear Cl···K^+···Cl arrangement and showing the 65.15° rotation; (b) the Cl–Au–Cl···K^+ 'spine' in the *C*2/*c* polymorph of **3**, illustrating the linear arrangement of the potassium cations; (c) the linear arrangement of potassium ions in the $P2_1/n$ polymorph (crown ethers removed in all views for clarity).

In considering the transformation from gold(III) (**2**) to gold(I), it is instructive to observe the two structures that co-exist during the data collection (Fig. 9). This shows that while the position of the crown ethers is invariant, irradiation leads to some randomization of the position of gold(III) centers and reduction to gold(I), the latter accompanied by a significant displacement of the gold center by 1.5 Å into a linear coordination environment, accompanied by a lengthening of the Au–Cl bonds from 2.26 Å in gold(III) to 2.33(1) Å in gold(I) and some lateral movement. This is consistent with a reductive elimination of Cl_2 leaving a gold(I) center displaced to accommodate the new coordination geometry, although it is not really possible to speculate on a mechanism by which this might occur. That said, as mentioned already extensive radiation-induced transformation to the gold(I) complex does lead the crystal to degrade over time and it is possible that this may reflect the disruptive effect of the physical escape of gas molecules.

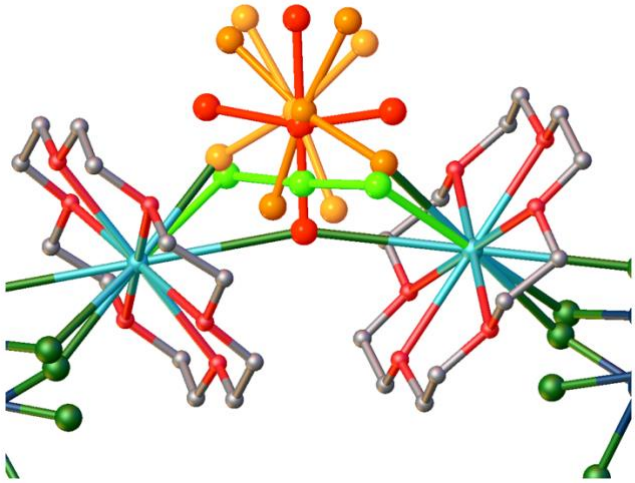

Figure 9 Overlaid structure of **2** and **3** from a cif obtained during data collection. The different disordered forms of $[AuCl_4]^-$ are shown in orange or red, while $[AuCl_2]^-$ is in lime green.

Conclusion

The present study shows what we believe to be a unique concurrence of events, namely that the newly reported potassium crown ether salt of tetrachloroaurate(III) first undergoes a rapid and reproducible, non-epitaxial single-crystal-to-single-crystal transition from a *P*–1 to a *C*2/*c* polymorph. The transition appears driven by some randomization of the rotational position of the square-planar gold(III) center about an axis perpendicular to the anion plane. That the transition is rapid is demonstrated by the fact that it is difficult to obtain a complete data collection on a crystal in the *P*–1 space group as very rapid data collection is required. Crystals are recovered with no sign of damage or rupture.

However, values of R_1 obtained from fitting data sets where crystals had been irradiated for extended periods gave rather high values for R_1 (**1b** – 10.54%; **1c** – 13.17%) and there was evidence of significant electron density associated with gold and chlorine that was unaccounted. Modelling this at different proportions of $[AuCl_2]^-$ caused R_1 to drop significantly (to 8.75% and 3.26%, respectively), revealing a photoinduced, two-electron reduction to [K(18-crown-6)][$AuCl_2$]. Details of the nature of the reduction could not be elucidated in this study.

It then proved possible to extract a model for the gold(I) complex, which showed that it exists in the *C*2/*c* space group, in common with its gold(III) precursor so that the chemical change is effectively isomorphous. Furthermore, while the single crystal X-ray structure of [K(18-crown-6)][$AuCl_2$] has been reported previously,[12] it was in the $P2_1/n$ space group, meaning that a new polymorph has been realized.

Taken together, the sequence [K(18-crown-6)][$AuCl_4$] (*P*–1) to [K(18-crown-6)][$AuCl_4$] (C_2/c) to [K(18-crown-6)][$AuCl_2$] (C_2/c) represents a unique series of radiation-induced transformations.

Experimental

Materials

K[$AuCl_4$] was obtained as a loan from Johnson Matthey. [18-crown-6] was purchased from Sigma Aldrich. ^{1}H NMR spectrum was recorded on Jeol ECX300 (400 MHz). The elemental analysis was done for Exeter Analytical Inc., CE-440 Elemental Analyser.

For all crystals except **3**, the single crystal X-ray data were collected on an Oxford Diffraction SuperNova diffractometer using either MoKα radiation (λ = 0.71073 Å, for **1a**, **1b**, **2a** and **2b**) or Cu$K\alpha$ radiation (λ = 1.54184 Å, for **1c**). For **3**, data was collected using a Bruker Smart Apex diffractometer using MoKα radiation (λ = 0.71073 Å). For all the crystal was kept at 110 K during data collection. The structure was solved by using Olex2,[16] and solved with ShelXS[17] applying the direct methods (**1a**, **2a** and **2b**) or ShelXT[18] (**1b** and **1c**) and refined with the ShelXL[19] refinement package using least squares minimization.

Synthesis

To a solution of [18-crown-6] (0.50 mmol, 0.132 g) in water (2 cm^3) was added another solution of K[$AuCl_4$] (0.25 mmol, 0.0945 g) in water (2 cm^3) followed by stirring of the contents for 24 h in the

dark. A yellow precipitate was observed which was filtered off, washed with water (4 cm^3), EtOH (2 cm^3) and Et_2O (2 cm^3) and then dried under vacuum for 18 h. Yield: 84% (0.2099 mmol, 0.1348 g). The above reaction was also carried out in CH_3COOH:H_2O *i.e.* 1:1 (v/v %) to obtain the final structure of the complex *i.e.* [K(18-crown-6)][$AuCl_4$].

Analysis: Elemental, found (expected): C 22.3, H 3.7 % (C 22.4, H 3.8 %). ^{1}H NMR, 400 MHz, $CDCl_3$: δ3.66 (s). XRD (single crystals) from CH_2Cl_2: yellow crystals correspond to [K(18-cr-6)][$AuCl_4$] (major) and some colorless crystals were also obtained corresponding to [K(18-cr-6)][$AuCl_2$][5] (minor) determined by analysis of the unit cell.

Acknowledgements

We thank the Wild Fund of the Department of Chemistry, University of York, for support to NKS, Johnson Matthey for generous loans of K[$AuCl_4$] and Rachel Parker for re-preparing and crystallizing [K(18-crown-6)][$AuCl_4$].

References

1. L. E. Hatcher and P. R. Raithby, Dynamic single-crystal diffraction studies using synchrotron radiation, *Coord. Chem. Rev.*, 2014, **277-278**, 69-79.
2. X.-N. Cheng, W.-X. Zhang and X.-M. Chen, Single Crystal-to-Single Crystal Transformation from Ferromagnetic Discrete Molecules to a Spin-Canting Antiferromagnetic Layer, *J. Am. Chem. Soc.*, 2007, **129**, 15738-15739
3. Y. Abe, A. Karasawa and N. Koga, Crystal Structures and Emitting Properties of Trifluoromethylaminoquinoline Derivatives: Thermal Single-Crystal-to-Single-Crystal Transformation of Polymorphic Crystals That Emit Different Colors, *Chem. Eur. J.*, 2012, **18**, 15038-15048.

4. P. Kissel, D. J. Murphy, W. J. Wulftange, V. J. Catalano and B. T. King, A nanoporous two-dimensional polymer by single-crystal-to-single-crystal photopolymerization, *Nat. Chem.*, 2014, **6**, 774-778.

5. S. D. Pike, A. L. Thompson, A. G. Algarra, D. C. Apperley, S. A. Macgregor, A. S. Weller, Synthesis and Characterization of a Rhodium(I) σ-Alkane Complex in the Solid State, *Science*, 2012, **337**, 1648-1651.

6. F. M. Chadwick, A. I. McKay, A. J. Martinez-Martinez, N. H. Rees, T. Krämer, S. A. Macgregor and A. S. Weller, Solid-state molecular organometallic chemistry. Single-crystal to single-crystal reactivity and catalysis with light hydrocarbon substrates, *Chem. Sci.*, **2017**, *8*, 6014-6029; A. I. McKay, T. Kräïmer, N. H. Rees, A. L. Thompson, K. E. Christensen, S. A. Macgregor, and A. S. Weller, Formation of a σ-alkane Complex and a Molecular Rearrangement in the Solid-State: $[Rh(Cyp_2PCH2CH_2PCyp_2)(\eta^2{:}\eta^2\text{-}C_7H_{12})][BArF^4]$, *Organometallics*, 2017, **36**, 22−25.

7. A. Mori, N. Kato, H. Takeshita, Y. Kurahashi and M. Ito, X-Ray-induced Retro [2+2] Cycloaddition of a *syn*-Tricyclo[4.2.0.0^{2,5}]octane derivative to a *cis,cis*-Cycloocta-1,5-diene Derivative within a Single Crystal Lattice, *J. Chem. Soc.*, *Chem. Commun.*, 1994, 869-870.

8. A. Mori, T. Nakamura, K. Kubo, T. Hatsui, and N. Kato, Single Crystal-to-Single Crystal Transformation of a *syn*-Tricyclo[4.2.0.0^{2,5}]octane to a (*Z,Z*)-Cycloocta-1,5-diene under X-ray Irradiation, *Mol. Cryst. Liq. Cryst.*, 2002, **389**, 65-71.

9. Y. Sekine, M. Nihei, R. Kumai, H. Nakao, Y. Murakami, and H. Oshio, X-ray-induced phase transitions by selective excitation of heterometal ions in a cyanide-bridged Fe–Co molecular square, *Chem. Commun.*, 2014, **50**, 4050-4052.

10. N. K. Sethi, A. C. Whitwood and D. W. Bruce, Homo- and Hetero-bimetallic Complexes of TTHA, *Polyhedron*, 2012, **33**, 378-387.

11. N. K. Sethi, A. C. Whitwood, and D. W. Bruce, Preparation of a Heterodimetallic Di-μ-chlorido Complex of Palladium and Platinum, *Eur. J. Inorg. Chem.*, 2013, 2078-2082.

12. Md. A. Hossain, D. R. Powell, and K. B. James, A potassium crown ether complex with dichloroaurate(I), *Acta Cryst.*, 2003, **E59**, m57.

13. M. Calleja, K. Johnson, W. J. Belcher, J. W. Steed, Oxonium Ions from Aqua Regia: Isolation by Hydrogen Bonding to Crown Ethers, *Inorg. Chem.*, 2001, **40**, 4978-4985.

14. F. Wu, H. Tong, Z. Li, W. Lei, L. Liu, W.-Y. Wong, W.-K. Wong, X. Zhu, A white phosphorescent coordination polymer with Cu_2I_2 alternating units linked by benzo-18-crown-6, *Dalton Trans.*, 2014, **43**,12463.

15. X.-M. Song, X.-Q. Huang, J.-M. Dou, D.-C. Li, *catena*-Poly[[(18-crown-6)potassium(I)]-μ-chlorido-silver(I)-μ-chlorido], *Acta Cryst.*, 2007, **63E**, m2219.

16. O. V. Dolomanov, L. J. Bourhis, R. J. Gildea, J. A. K. Howard, and H. Puschmann, OLEX2: a complete structure solution, refinement and analysis program, *J. Appl. Cryst*., 2009, **42**, 339-341.

17. G.M. Sheldrick, A short history of SHELX, *Acta Cryst.*, 2008, **A64**, 112-122.

18. ShelXT – Integrated space-group and crystal-structure determination, G. M. Sheldrick, *Acta Cryst.*, 2015, **A71**, 3-8.

19. G. M. Sheldrick, Crystal structure refinement with SHELXL, *Acta Cryst.*, 2015, **C71**, 3-8.

Abstract:

During data collection, the unreported potassium crown-ether salt [K(18-crown-6][$AuCl_4$] undergoes a sequential, X-ray-induced and irreversible single-crystal-to-single-crystal transformation from *P*–1 to *C*2/*c* followed by a topotactic reduction to crystalline [K(18-crown-6][$AuCl_2$] within the same *C*2/*c* space group.

Graphic Abstract: